

# Parasitic Loaded Shorting Pin Based Compact Multi-slot LoRa Antenna for Military Application

Reeta Devi<sup>1\*</sup>, Pranjal Borah<sup>2</sup>, Santosh Kumar Prasad<sup>1</sup>

<sup>1</sup> Department of Physics, Dibrugarh University, Dibrugarh 786004, Assam, India

<sup>2</sup> Department of Instrumentation and USIC, Gauhati University, Jalukbari, Guwahati, Assam 781014, India

\* Corresponding author, e-mail: [reetadevi@dibru.ac.in](mailto:reetadevi@dibru.ac.in)

Received: 18 September 2023, Accepted: 07 March 2024, Published online: 24 May 2024

## Abstract

In this paper, work on a compact multi-slot patch antenna with a parasitic load and shorting-pin has been presented for its use in long range (LoRa) defense applications. Initially the antenna is designed and simulated using HFSS and a parametric study has been carried out for achieving an optimized antenna configuration. This is followed by the fabrication of antenna prototype based on the optimal performances obtained from the simulated results. Further, the return loss along with free space co-polar and cross-polar radiation pattern measurements has been carried out for the fabricated antenna. The experimental results show a good comparison with that of the simulated one. The proposed antenna resonates at an operating frequency of 866 MHz, providing a -10 dB bandwidth from 856 MHz-877 MHz, which covers the wireless standard used for LoRa technology. Finally, a comparative analysis of the proposed antenna with the recently reported works is presented.

## Keywords

compact, shorting pin, parasitic strip, LoRa

## 1 Introduction

Long Range (LoRa) band is specially defined for an efficient communication range that ascertains a good connectivity among the different module of IoT network. Undoubtedly, antenna design and its working in the LoRa band plays a vital role in this communication field [1]. Moreover, reported works show that the use of antenna in the defense system has gained a lot of interests among the researchers [2–5]. In the diverse IoT environment such as in the battle fields, the major demand for an antenna is the compactness in size. Microstrip patch antennas with the features like compatibility, low profile and easy to integrate are hence preferred for such IoT applications. In recent years, a lot of antennas working in different IoT environment as well as LoRa technology have been reported [6–14]. An inverted F-antenna for IoT devices using LoRa technology is designed for a single resonating frequency band in [6]. A CubeSat microstrip antenna with metamaterial structure is proposed for LoRa communication in [7]. In [9], a dual-band conductive textile-based wearable antenna operating at LoRa and Bluetooth range is proposed for application in accurate geolocation, tracking and communication in the military and telemedicine

industries. In [10] various techniques for miniaturization of antenna are reported with a proposed inset fed rectangular microstrip antenna resonating at LoRa band. In [11], a dual-band footwear textile antenna is presented for off-body network communication, which can be applicable for LoRa applications covering 433 MHz, 868 MHz and 915 MHz bands. However, the size of the antenna is still a factor to be concerned. Many techniques have been explored in the literature for the miniaturization of multi-band antennas such as defected ground structure [15–17], slotting [18–23] and parasitic loading [24, 25] etc. The use of shorting pins is one of the favorite techniques used for antenna design because of their planar profile, ruggedness and ease of fabrication. In recent years, it has been used extensively for reducing the size of the patch [26–29].

In this work, we propose a compact microstrip patch antenna for its possible use in wearable defense application working in the LoRa band. The proposed antenna has an impedance bandwidth of 21 MHz (856–877) MHz that covers LoRa band. Three simple techniques of size reduction such as shorting pin, slot loaded patch and parasitic element have been adopted altogether for this design

where a reduction of 93% has been achieved. Further, being miniature in size the proposed antenna is suitable to be integrated with the bullet proof armor of the soldier.

## 2 Antenna design and parametric analysis

The working of the proposed antenna is based on the effective shunt inductance property of shorting pin and effective electrical length property of slot to reduce the frequency of operation. At first, the antenna is designed and simulated using HFSS where the final geometry of the antenna evolves out after a few succeeding steps and thereby it is targeted to achieve a better matching result in the required band of operation. FR-4 material of thickness 1.5 mm is used as the dielectric substrate for the design where a linear array of slots at equidistant position has been introduced over a rectangular patch of length 46 mm and width 13 mm. This is followed by incorporation of a shorting pin near to the co-axial probe feed location of the patch. Afterwards, the array of slots is made inclined downward at angle of 30° without changing the feed point and the shorting pin position of the antenna. Subsequently, the opening edge of the slots has been truncated which are finally shorted via a parasitic microstrip line, as shown in Fig. 1.

Fig. 2 shows the simulated matching performances at the various steps of the antenna design.

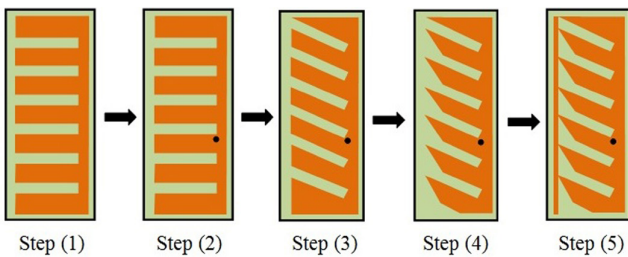


Fig. 1 Step by step procedure for designing the antenna

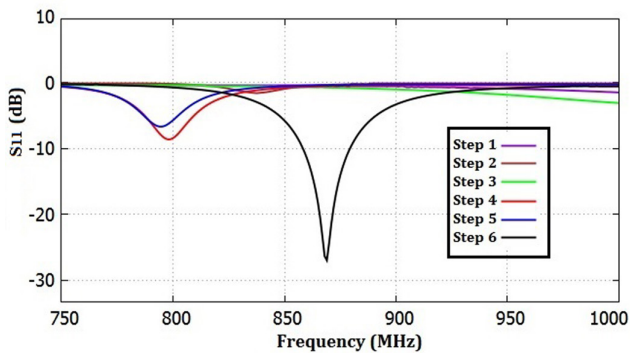


Fig. 2 Simulated return loss plots at different steps of the antenna design

It can be seen that the introduction of the shorting pin in the rectangular patch having inclined array of slots shows a trend of matching nearby 800 MHz. Further, the addition of the parasitic line on the truncated open edge of the slots allows the antenna to have a good matching at the frequency of interest at around 870 MHz. A parametric analysis has been carried out via simulation for obtaining an optimal antenna configuration that aims for its operation in the required band. This analysis is also opted to have an insight of the effect on the antenna matching performances due to change in its different design parameters by keeping the feed point location fixed throughout the analysis. Fig. 3 shows the schematic diagram of the final design of the proposed antenna.

### 2.1 Effect of shorting pin location ( $x_p, y_p$ ) and the parasitic linewidth ( $p$ )

The effect of the shorting pin positions along with the parasitic line width on the matching performance has been observed by keeping the feed point constant ( $x_f = 37.5$  mm,  $y_f = 3$  mm) and the dimension of the slot length ( $S_L$ ) and width ( $S_W$ ) at a fixed value of 11 mm and 2 mm respectively. To maintain the compactness of the proposed design, the ground plane dimension is initially maintained at  $L_g = 48$  mm and  $W_g = 15$  mm. The simulated return loss performances for different feed position ( $x_p, y_p$ ) and the parasitic line width ( $p$ ) are shown in Fig. 4 (a, b, c).

It can be seen that, for the opted feed point location and the dimension of  $S_L$  and  $S_W$ , a better matching performance is obtained for the shorting pin location at  $x_p = 31$  mm and  $y_p = 3$  mm for all the antenna configurations having different parasitic line width ( $p$ ). However, amongst the three different parasitic line width configurations, a suitable result is seen for  $p = 0.5$  mm and  $x_p = 31$  mm and  $y_p = 3$  mm with a S11 value of  $-40.10$  dB at 866 MHz.

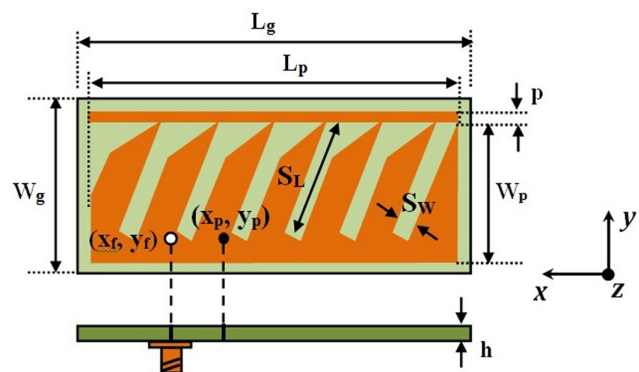
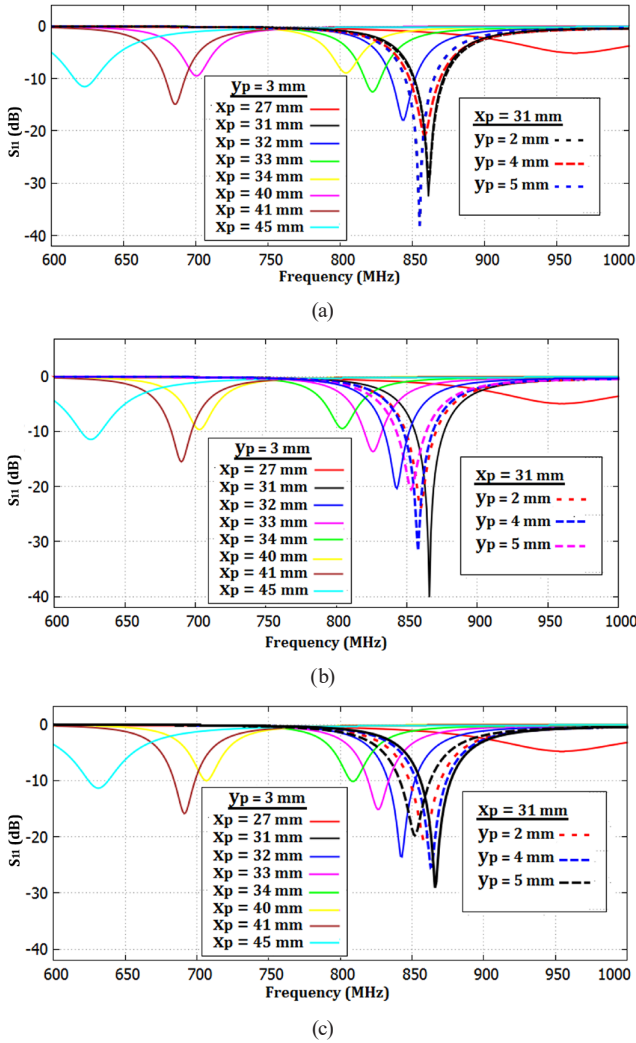


Fig. 3 Schematic diagram of the final design of the proposed antenna



**Fig. 4** (a) Simulated S11 plot for different feed position ( $x_p, y_p$ ) with the parasitic line width ( $p = 0.3$  mm); (b) Simulated S11 plot for different feed position ( $x_p, y_p$ ) with the parasitic line width ( $p = 0.5$  mm); (c) Simulated S11 plot for different feed position ( $x_p, y_p$ ) with the parasitic line width ( $p = 0.8$  mm)

## 2.2 Effect of slot length ( $S_L$ ) and slot width ( $S_W$ )

To have an insight of the effect of  $S_L$  and  $S_W$  on the antenna matching performance, simulations are carried out by varying its dimensions whereas the other parameters are maintained at a value that provides the best matching performance in the preceding analysis. The slot length  $S_L$  is varied from 10 mm to 12 mm in steps of 1 mm whereas the slot width is varied from 1 mm to 2.5 mm in steps of 0.5 mm. The simulated S11 plots for different values of  $S_L$  and  $S_W$  are shown in Fig. 5.

From the obtained simulated results, it can be seen that the slot width  $S_W$  has a greater impact on the operating frequency of the antenna whereas an increase in  $S_W$  shift the resonating frequency to the lower side of the RF spectrum. Apart from the slot length  $S_L = 2.5$  mm, rest

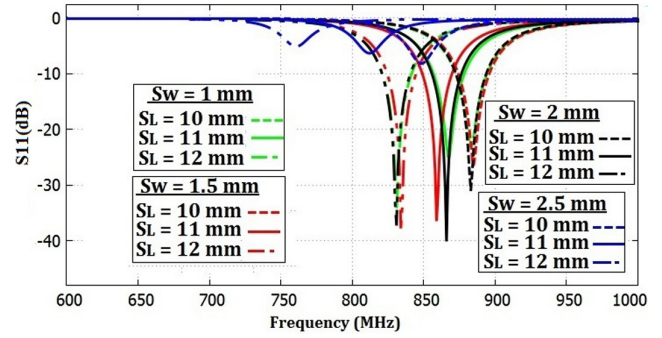


**Fig. 5** Simulated S11 plots for different values of  $S_L$  and  $S_W$

shows a minimum variation in the resonant frequencies and in their corresponding S11 values. However, the best matching is obtained for the antenna configuration having  $S_L = 11$  mm and  $S_W = 2$  mm.

## 2.3 Effect of ground plane ( $L_g \times W_g$ )

Simulations are carried out by varying the ground plane dimension ( $L_g \times W_g$ ) of the antenna to have an insight of its effect on the antenna matching performances where the rest of the parameters are fixed at their optimal dimensions obtained from the preceding observations. The simulated return loss plots are shown in Fig. 6 with three different values of  $L_g$  and  $W_g$ .

As can be seen, with the increase in the ground plane width  $W_g$ , the resonant frequency of the antenna is shifted to lower side of the RF spectrum. Further, it has been observed that for a given dimension of  $W_g$ , the resonant frequency of the antenna shifts towards the higher side of the RF spectrum with increment in the ground plane length  $L_g$ . Among all the variations, simulated results show a better matching for the antenna configuration having  $L_g = 48$  mm and  $W_g = 15$  mm.

## 3 Experimental results

From the parametric analysis that has been carried out, the antenna prototype is fabricated using the optimal

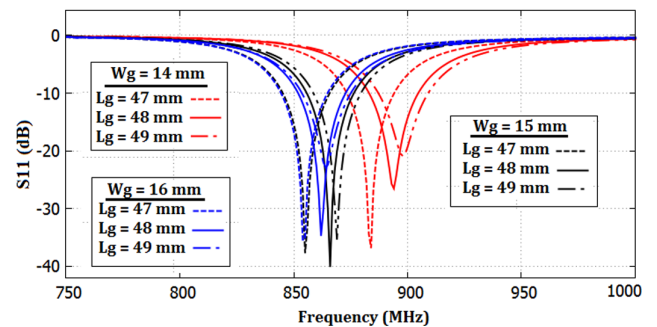


**Fig. 6** Simulated S11 plots for different values of  $L_g$  and  $W_g$

dimensions as shown in Table 1 and the fabricated antenna is shown in Fig. 7. Return loss and radiation pattern measurements are carried out and the results are compared with that of the simulated one.

### 3.1 Return loss measurement

The return loss measurement of the fabricated antenna is carried out by using a vector network analyzer (Rohde & Schwarz ZNB20). The measurement is also taken by mounting the antenna on a Kevlar material to have an insight of its effect on the matching performances when shall be mounted on the military tactical vest in the battle ground. Moreover, the antenna is covered with radome like material to eliminate the environmental effects and this is followed by the return loss measurement to observe the effect of the material on the antenna performance. The simulated and measured return loss plots for the proposed antenna are shown in Fig. 8. It is observed that the simulated and measured results are in good agreement.

Although, a small shift in the resonant frequency for the antenna mounted on the Kevlar material is observed which may be due to the fabrication tolerances but the operational  $-10$  dB bandwidth lies in the required LoRa band of operation. Also, there are no significant changes in its return loss value and  $-10$ dB bandwidth when the designed antenna is covered by plastic radome like material. However, the radome material must be chosen carefully as it may reduce the radiation efficiency of the antenna. Table 2 shows the simulated and the measured return loss values at their corresponding resonant frequencies.

### 3.2 Radiation pattern measurement

The free space co-polarization and cross-polarization radiation pattern measurements of the single antenna are carried out using DAMS antenna measurement setup where the vector network analyzer is interfaced with a computer along with an automated turn table. The measured and simulated radiation patterns at their corresponding resonant frequencies are shown in Fig. 9 (a, b).

It can be seen that both the x-z and y-z plane show a broad-side radiation pattern whereas the cross-polarization levels lie below  $-10$  dB at its corresponding co-polar maximum. The measured gain at the resonant frequency of the proposed antenna comes out to be around 1.5 dBi as provided by the

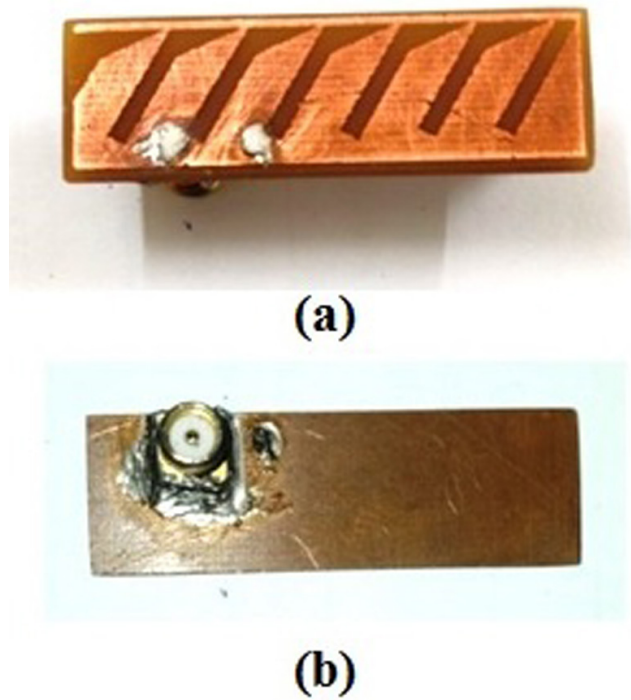


Fig. 7 Fabricated antenna (a) top and (b) bottom view

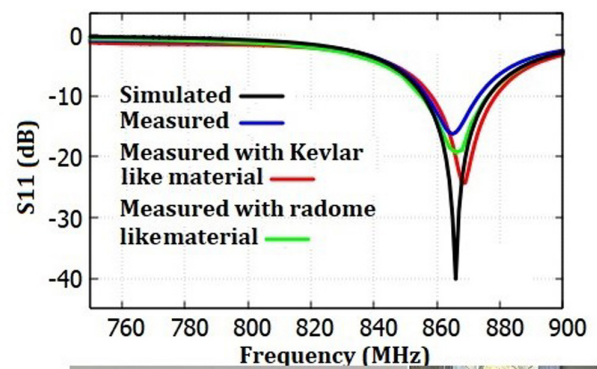


Fig. 8 Simulated and measured return loss plots of the proposed antenna

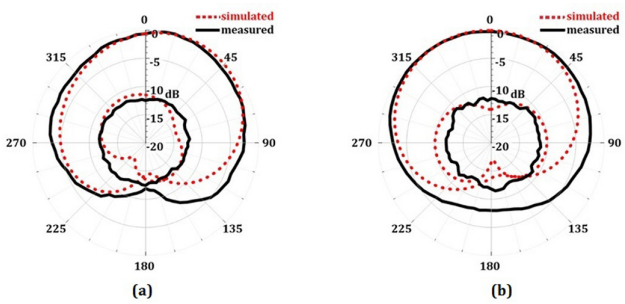
DAMS antenna measurement setup. The radiation pattern so obtained can also be verified from the surface current distribution at 866 MHz which is shown in Fig. 10.

Table 1 Optimized designed parameters of the proposed antenna

Ref [Fig 3]	Parameters	$L_g$	$W_g$	$L_p$	$W_p$	$p$	$S_L$	$S_W$	$(x_p, y_p)$	$(x_r, y_r)$
	Value (mm)	48	15	46	13	0.5	7	2.7	(37.5, 3)	(31, 3)

**Table 2** Simulated and measured S11 values at their corresponding resonant frequencies

Antenna configuration	S11 (dB)	Frequency (MHz)
Simple	Simulated	-40.10
	Measured	-16.25
Measured with Kevlar material	-24.35	868
Measured with radom like material	-18.82	865



**Fig. 9** Simulated and measured radiation pattern in (a) x-z plane; (b) y-z plane

### 3.3 Antenna size reduction calculation

The dimension of a conventional rectangular patch working in the LoRa band (856–877 MHz) designed on FR-4 substrate having thickness of 1.5 mm generally has a dimensional area of  $105 \times 82 \text{ mm}^2$  whereas this proposed design has an overall occupied patch area of  $46 \times 13 \text{ mm}^2$ . The total size reduction thus can be found by the Eq. (1),

$$(A - B) / A \times 100\%, \tag{1}$$

where  $A$  is the original dimension and  $B$  is the reduced dimension. By placing the values  $A = 105 \times 82 \text{ mm}^2$  and  $B = 46 \times 13 \text{ mm}^2$  an overall size reduction of 93% has been achieved.

### 4 Discussions and conclusion

A compact antenna loaded with shorting pin, slot and parasitic patch is presented in this paper. The proposed antenna has an overall dimension of  $48 \times 15 \times 1.5 \text{ mm}^3$  including the ground plane. The antenna shows an impedance bandwidth of 21 MHz covering the LoRa band for long range communications. Geometrically, the truncated inclined slots along with the shorting pin and the parasitic line for the chosen feed position provides the overall size reduction of around 93% than the conventional rectangular patch dimension by

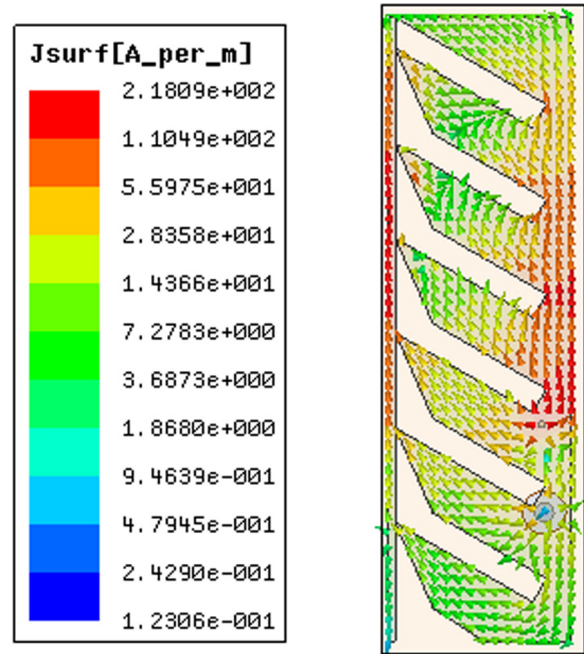


**Fig. 10** Surface current distribution of the proposed antenna at 866 MHz

increasing the electrical length. Being miniature in size and the obtained measured results, the proposed antenna can be a potential candidate in LoRa communication system. Further, it can also be mounted on military armor for sharing information such as data obtained from mine detectors among the military troops and their headquarters. This will help the military to decide the future movement of troops from the area; mines removing missions and marking the areas as landmine danger zones. The antenna is also found to be satisfactory in its performance whenever covered with radome like materials to protect it from external environmental effects. A performance comparison has been carried out between the proposed antenna and others related works as shown in Table 3. It shows that that the proposed antenna is satisfactory one in terms of impedance bandwidth and size.

### Acknowledgement

The authors thankfully acknowledge the support provided by Department of Science & Technology (DST), India, in terms of FIST supported experimental set up at Department of Physics, Dibrugarh University. The authors are also grateful to the Department of Instrumentation and USIC and Department of Electronics and Communication Technology, Gauhati University for their kind support.

**Table 3** Comparative analysis of the proposed antenna with reported work

Ref.	Substrate	Size (in mm <sup>3</sup> )	Bandwidth (in MHz)	Technique used
[6]	FR-4	34× 80× 0.8	847-873	IFA
[7]	FR-4	250 × 250 × 19.6	758-983	Metamaterial
[8]	FR4	120 × 120 × 0.8	791-1123	Meander line
[9]	Neoprene	150 × 150 × 3.2	863-870	Aperture coupled
[10]	FR4	67.74 × 55 × 1.58	857-885	Inset fed, ground etching
[11]	Metal and wool	95 × 65 × 25	433, 868 and 915	flexible textile
Proposed antenna	FR-4	48 × 15 × 1.5	856-877	Shorting Pin, parasitic element

## References

- [1] Sondrol, T., Jalaian, B. Suri, N. "Investigating LoRa for the Internet of Battlefield Things: A Cyber Perspective", In: MILCOM 2018, IEEE Military Communications Conference (MILCOM), Los Angeles, CA, USA, 2018. pp. 749–756. ISBN 9781538671856 <https://doi.org/10.1109/MILCOM.2018.8599805>
- [2] Borah, P., Das, D. "Three dimensional star antenna for wearable defense application", Microwave and Optical Technology Letters, 64(10), pp. 1779–1784, 2022. <https://doi.org/10.1002/mop.33339>
- [3] Lee, H., Tak, J., Choi, J. "Wearable Antenna Integrated into Military Berets for Indoor/Outdoor Positioning System", IEEE Antennas and Wireless Propagation Letters, 16, pp. 1919–1922, 2017. <https://doi.org/10.1109/LAWP.2017.2688400>
- [4] Shin, J.-Y., Woo, J. "Military Antennas", In: International Symposium on Antennas and Propagation (ISAP), Busan, South Korea, 2018, pp. 1–2. ISBN 9788957082973
- [5] Venugopal, K., Heath, R. W. "Millimeter Wave Networked Wearables in Dense Indoor Environments", IEEE Access, 4, pp. 1205–1221, 2016. <https://doi.org/10.1109/ACCESS.2016.2542478>
- [6] Trinh, L. H. Nguyen, T. Q. K., Phan, D. D., Tran, V. Q., Bui, V. X., Truong, N. V., Ferrero, F. "Miniature antenna for IoT devices using LoRa technology", In: International Conference on Advanced Technologies for Communications (ATC), Quynhon, Binh Dinh Province, Vietnam, 2017, pp. 170–173. ISBN 9781538628966 <https://doi.org/10.1109/ATC.2017.8167611>
- [7] Putra, N. A. H., Edward, Hasbi, W., Manggala, M. P., Kusmara, D. U., Putri, W. M., Triyogi, R., Wirakusama, M. P. "Design of Cubesat Microstrip Antenna with Metamaterial Structure for LoRa Communication", In: IEEE International Conference on Aerospace Electronics and Remote Sensing Technology (ICARES), Bali, Indonesia, 2021, pp. 1–5. ISBN 9781665401807 <https://doi.org/10.1109/ICARES53960.2021.9665185>
- [8] Wang, Z., Fang, S., Fu, S., Jia, S. "Single-Fed Broadband Circularly Polarized Stacked Patch Antenna with Horizontally Meandered Strip for Universal UHF RFID Applications", IEEE Transactions on Microwave Theory and Techniques, 59(4), pp. 1066–1073, 2011. <https://doi.org/10.1109/TMTT.2011.2114010>
- [9] Ibrahim, N. F., Dzabletey, P. A., Kim, H., Chung, J.-Y. "An All-Textile Dual-Band Antenna for BLE and LoRa Wireless Communications", Electronics, 10(23), 2967, 2021. <https://doi.org/10.3390/electronics10232967>
- [10] Pandey, A., Deepak Nair, M. V. "Inset Fed Miniaturized Antenna with Defected Ground Plane for LoRa Applications", Procedia Computer Science, 171, pp. 2115–2120, 2020. <https://doi.org/10.1016/j.procs.2020.04.228>
- [11] Huang, R., Xia, W., Xing, L., Zhu, F. "A Dual Band Footwear Textile Antenna for LoRa Off-Body Communication", In: 2022 IEEE Conference on Antenna Measurements and Applications (CAMA), Guangzhou, China, 2022, pp. 1–4. ISBN 9781665490382 <https://doi.org/10.1109/CAMA56352.2022.10002504>
- [12] Masius, A. A., Wong, Y. C., Lau, K. Y. "Miniature high gain slot-fed rectangular dielectric resonator antenna for IoT RF energy harvesting", AEU – International Journal of Electronics and Communications, 85, pp. 39–46, 2018. <https://doi.org/10.1016/j.aeu.2017.12.023>
- [13] Kulkarni, P., Srinivasan, R. "Compact polarization diversity patch antenna in L and WiMAX bands for IoT applications", AEU - International Journal of Electronics and Communications, 136, 153772, 2021. <https://doi.org/10.1016/j.aeu.2021.153772>
- [14] Maurya, N. K., Bhattacharya, R. "Design of compact dual-polarized multiband MIMO antenna using near-field for IoT", AEU - International Journal of Electronics and Communications, 117, 153091, 2020. <https://doi.org/10.1016/j.aeu.2020.153091>
- [15] Mark, R., Mishra, N., Mandal, K., Sarkar, P. P., Das, S. "Hexagonal ring fractal antenna with dumb bell shaped defected ground structure for multiband wireless applications", AEU - International Journal of Electronics and Communications, 94, pp. 42–50, 2018. <https://doi.org/10.1016/j.aeu.2018.06.039>
- [16] Chen, W. Yao, Y., Yu, J., Liu, X., Chen, X. "Design of a novel multiband antenna for mobile terminals", In: IEEE International Wireless Symposium, Shenzhen, China, 2015, pp. 1–4. ISBN 978-1-4799-1928-4 <https://doi.org/10.1109/IWSS.2015.7164622>
- [17] Al-Mihrab, M. A., Salim, A. J., Ali, J. K. "A Compact Multiband Printed Monopole Antenna with Hybrid Polarization Radiation for GPS, LTE, and Satellite Applications", IEEE Access, 8, pp. 110371–110380, 2020. <https://doi.org/10.1109/ACCESS.2020.3000436>

- [18] Das, T. K., Dwivedy, B., Behera, K. S. "Design of a meandered line microstrip antenna with a slotted ground plane for RFID applications", *AEU - International Journal of Electronics and Communications*, 118, 153130, 2020.  
<https://doi.org/10.1016/j.aeue.2020.153130>
- [19] Hussain, R., Khan, M. U., Sharawi, M. S. "An Integrated Dual MIMO Antenna System with Dual-Function GND-Plane Frequency-Agile Antenna", *IEEE Antennas and Wireless Propagation Letters*, 17(1), pp. 142–145, 2018.  
<https://doi.org/10.1109/LAWP.2017.2778182>
- [20] Devi, R., Neog, D. K. "Wideband dual frequency antenna for WLAN applications", In: *IEEE Applied Electromagnetic Conference (AEMC)*, Kolkata, India, 2011, pp. 1–4. ISBN 978-1-4577-1098-8  
<https://doi.org/10.1109/AEMC.2011.6256776>
- [21] Devi, R., Neog, D. K. "A Compact Elevated CPW-fed Antenna with Slotted Ground Plane for Wideband Applications", *International Journal of Microwave and Wireless Technologies*, 9(10), pp. 2005–2011, 2017.  
<https://doi.org/10.1017/S1759078717000915>
- [22] Kashyap, P., Sharma, K., Dakua, I., Baruah, S. "Gain and bandwidth enhancement of slotted microstrip antenna using metallic nanofilms for WLAN applications", *Journal of King Saud University – Science*, 35(1), 102374, 2023.  
<https://doi.org/10.1016/j.jksus.2022.102374>
- [23] Devi, R., Neog, D. K. "Wideband planar slot antenna with a pair of E-shaped parasitic patches for wireless applications", In: *3<sup>rd</sup> International Conference on Signal Processing and Integrated Networks (SPIN)*, Noida, Delhi NCR, India, 2016, pp. 596–599. ISBN 9781467391986  
<https://doi.org/10.1109/SPIN.2016.7566766>
- [24] Sim, C.-Y.-D., Yeh, C.-H., Lin, H.-L. "Compact size triple-band monopole antenna with parasitic element for WLAN/WiMAX applications", In: *International Symposium on Antennas and Propagation Conference Proceedings*, Denver, CO, USA, 2014, pp. 469–470. ISBN 978-9-8691-4740-8  
<https://doi.org/10.1109/ISANP.2014.7026730>
- [25] Li, Y.-N., Chu, Q.-X. "Compact Eight-Band Monopole for LTE Mobile Phone", In: *14<sup>th</sup> European Conference on Antennas and Propagation (EuCAP)*, Copenhagen, Denmark, 2020, pp. 1–3.  
<https://doi.org/10.23919/EuCAP48036.2020.9135551>
- [26] Abolade, J. O., Konditi, B. O. "A shorting pin based compact meander multiband printed monopole antenna", *Heliyon*, 7(11), pp. 1–7, 2021.  
<https://doi.org/10.1016/j.heliyon.2021.e08390>
- [27] Ray, M. K., Mandal, K. "Shorting Pin and Slot Loaded Dual Band Microstrip Antenna for MICS and GPS Applications", In: *IEEE Indian Conference on Antennas and Propagation (InCAP)*, Hyderabad, India, 2018, pp. 1–4. ISBN 9781538670613  
<https://doi.org/10.1109/INCAP.2018.8770851>
- [28] Mir, R., Dashti, H., Ahmadi-Shokouh, J. "Design and analysis of circularly polarized circular patch antenna with multiple shorting pins using characteristic mode theory", *AEU - International Journal of Electronics and Communications*, 146, 154112, 2022.  
<https://doi.org/10.1016/j.aeue.2022.154112>
- [29] Shah, A., Patel, P. "Suspended embroidered triangular e-textile broadband antenna loaded with shorting pins", *AEU - International Journal of Electronics and Communications*, 130, 153573, 2021.  
<https://doi.org/10.1016/j.aeue.2020.153573>